Hindawi
Advances in Materials Science and Engineering
Volume 2022, Article ID 4901879, 13 pages
https://doi.org/10.1155/2022/4901879

Research Article

High-Temperature Rheology Characteristics of Hard Petroleum Asphalt Used in China

Bo Li,[1] **Binghui Wang**,[1] **Xijun Zhang**,[1] **Xixiong Lin**,[2] **and Yan Zhang**[1]

[1]*Key Laboratory of Road & Bridge and Underground Engineering of Gansu Province, Lanzhou Jiaotong University, Lanzhou 730070, China*
[2]*PetroChina Karamay Petrochemical Co. Ltd., Karamay, Xinjiang 834003, China*

Correspondence should be addressed to Bo Li; libolzjtu@hotmail.com

Received 24 November 2021; Accepted 13 January 2022; Published 15 February 2022

Academic Editor: Carlo Santulli

Hard petroleum asphalt, which is a high modulus asphalt binder material, is used for improving asphalt pavement rutting distress. This property is attributed to the good high-temperature rheological characteristics of hard petroleum asphalt. The study investigates the performance of hard petroleum asphalt and Styrene-Butadiene-Styrene polymer modified asphalt (SBSPMA) based on three aspects: asphalt oil source, asphalt grade, and aging degree. The short-term and long-term aging of four hard petroleum asphalts and SBSPMA of comparative samples were measured using the rolling thin film oven test (RTFOT) and the pressure aging test (PAV). Firstly, the viscosity-temperature curve of hard petroleum asphalt was obtained using the Brookfield viscosity test at different temperatures combined with the improved REFUTAS formula. The complex shear modulus (G^*), phase angle (δ), and rutting factor ($|G^*|/\sin\delta$) of each asphalt sample were then measured by the dynamic shear rheometer test (DSR). Furthermore, the temperature sensitivity of each asphalt sample was calculated using the complex modulus index method (GTS). The compaction and paving temperature ranges of each asphalt were then confirmed. The results showed that the high-temperature rheological characteristics of hard petroleum asphalt were similar to those of SBSPMA. The temperature sensitivity of hard petroleum asphalt was basically the same as that of SBSPMA, while the influence of aging on the G^* of hard petroleum asphalt was greater than that of SBSPMA. In addition, the hard petroleum asphalt construction temperature was lower than that of SBSPMA.

1. Introduction

With the continuous and rapid development of China's economy, the total mileage of existing highways has steadily increased [1]. However, during the maintenance of the pavement, more and more rutting distress has appeared at the entrance of highways and urban road intersections in China [2, 3]. Asphalt pavement rutting is caused by the shear resistance of asphalt pavement decreases in hot weather, and the reason for this condition is the low thickness and low load bearing capacity in the early design of asphalt pavement. As the total traffic volume and proportion of heavy vehicles increases, the pavement produces increasingly more rutting distress [4, 5]. The asphalt surface layer is also prone to rutting caused by the small permanent deformation capacity of the semirigid base [6, 7].

In response to the previously mentioned factors, academics have suggested many possible solutions through continuous research, which has shown that asphalt binder materials can contribute approximately 40% and aggregates can contribute 60% in the rutting resistance performance of the mixture from the perspective of raw materials [8]. High viscosity asphalt and high modulus asphalt can significantly improve the high-temperature performance of asphalt mixtures [9–12]. Also, the asphalt mixture can reduce the rutting distress of asphalt pavements by adding antirutting agents, which have primarily achieved the prevention of asphalt pavement rutting distress by improving the shearing strength of the asphalt mixture [13, 14]. Thirdly, rutting distress can be solved by improving the actual structure of the asphalt pavement [15]. However, these methods require a greater economic investment and higher technical level to

be supported. Therefore, a cheaper material with excellent rutting resistance is sought in order to improve the overall asphalt pavement rutting resistance.

In recent years, studies have shown that the use of hard petroleum asphalt obtained directly through petroleum refining is the least expensive and most effective measure to be taken. This method can improve the rutting resistance and increase the service life of asphalt pavement [16], and it has both relatively low penetration grade and excellent high-temperature performance. Compared with SBS modified asphalt, it also has good application prospects without adding special additives and having to undergo a complicated manufacturing process. Over the past several decades, the utilization of asphalt with high modulus in pavement has become an acceptable practice in many countries. In their research of hard petroleum asphalt mixtures, Brown et al. [17–19] used the linear elasticity theory in order to study fatigue cracking and the permanent deformation of hard petroleum asphalt mixtures by combining the effects of temperature and load. Hafeez et al. [20] compared six mixtures prepared by three kinds of the hard petroleum asphalt with the modified asphalt mixture. The high-temperature permanent deformation and permanent deformation coefficient of hard petroleum asphalt mixture was the same as those of modified asphalt. Garba [21–23] investigated the influence of load, temperature, and mixture type on the permanent transformation of hard petroleum asphalt mixture, and through a triaxial test and a creep recovery test, the prediction model and method for determining the permanent deformation of the hard petroleum asphalt mixture were obtained. Ouyang et al. [24] proposed the improvement of asphalt pavement rutting by enhancing the modulus of the asphalt mixture, and the results showed that the application of hard petroleum asphalt to intermediate layers could maximize the reduction of pavement rutting. Wu et al. [25] tested the dynamic modulus and fatigue parameters of asphalt mixture with high modulus (AC20, Sup20, and EME20) prepared hard petroleum asphalt, based on LPC asphalt mixture design guidelines.

In the area of hard petroleum asphalt research, Dong et al. [26] investigated the effects of SBS/CR on the high-temperature damage temperature and temperature sensitivity of hard-graded asphalt and found that the addition of SBS/CR to hard-graded asphalt could reduce the compaction temperature, enhance the temperature sensitivity, and strengthen the high-temperature fatigue resistance of the mixture. Xin et al. [27] selected SBSPMA, TLA, and NES-1 in order to modify the hard petroleum asphalt and obtained the regression equation between each component and the high-temperature performance of hard petroleum asphalt through a viscosity test and a softening point test. Sha et al. [28, 29] evaluated the high-temperature performance of two kinds of 50# hard petroleum asphalt through a DSR test, and the results showed that the shear and deformation resistance of hard petroleum asphalt mixture were excellent, while the penetration index was difficult to correctly assess for high-temperature performance. In summary, a relatively large number of studies have been carried out regarding the high-temperature properties of hard petroleum asphalt. The high-temperature performance of hard petroleum asphalt and hard petroleum asphalt mixes from various angles and methods has also been studied. However, there has been no comparative analysis of the rheological parameters of hard petroleum asphalt before and after aging, and the temperature sensitivity of hard petroleum asphalt at high temperatures remains unclear.

In this study, frequency sweep and temperature sweep were employed in order to interpret the high-temperature rheology characteristics of hard petroleum asphalt and SBSPMA at different aging levels. The index of GTS was carried out to evaluate the temperature sensitivity of hard petroleum asphalt, and the viscosity-temperature curves were obtained by a Brookfield viscosity test at different temperatures. The purpose of this study was to evaluate the high-temperature performance and to provide the applicable range of hard petroleum asphalt in order to guide the promotion of hard petroleum asphalt application.

2. Materials and Methods

2.1. Test Materials. The source of Kelian (KL) hard petroleum asphalt was Karamay, while the Gaofu (GF) hard petroleum asphalt was from Venezuela, and SBSPMA was provided by Gansu Road and the Bridge Research and Development Center. The asphalt includes Kelian, with a penetration grade of 20/40 and 40/60, and Gaofu, with penetration grades of 20/40 and 40/60, as well as SBSPMA. In order to facilitate the description, the asphalts were named K1, K2, G1, G2, and S1, respectively. The indexes of asphalt samples meet the requirements of standard demands (JTG E20-2011) [30, 31], and the basic performance is shown in Table 1.

2.2. Aging Test. When asphalt pavement is exposed to the air for long periods of time, it is subjected to the coupling effects of oxygen, ultraviolet light, and ozone. This causes the lighter components of the asphalt to volatilize and the adhesion properties of the asphalt to decay, and then the asphalt pavement subsequently produces cracks, looseness, spalling, and other types of distress. Therefore, the aging of asphalt is one of the key factors to determining the durability of asphalt pavement. Asphalt mixture in the mixing, transportation, and paving processes of aging is called short-term aging, while asphalt in the asphalt pavement service process of aging is called long-term aging.

2.2.1. Short-Term Aging. The SHRP plan proposes to use the RTFOT in order to carry out the short-term aging of asphalt. In this study, the temperature of RTFOT was 163°C ± 0.5°C, and the aging time was 85 minutes, according to ASTM D 2872.

2.2.2. Long-Term Aging. A PAV test is widely used to simulate the aging of asphalt in service. In this work, the test temperature was 100 ± 0.5°C, the aging time was 20h, and the test pressure was 2.10 ± 0.10 MPa, according to ASTM D 6521.

Table 1: Properties of asphalt.

Asphalt type	Penetration (25°C)/0.1 mm	Softening point/°C	Flash point/°C	Ductility (15°C)/cm	Density (25°C)/g/cm^3
K1	33.5	56.2	325	7.0	1.020
K2	51.7	52.7	315	21.3	1.035
G1	30.5	58.6	306	3.7	1.034
G2	44.7	52.5	290	28.6	1.081
S1	69.3	65.5	232	116.4	1.139

2.3. Brookfield Viscosity. The viscosity of asphalt can reflect the rheological properties and shear resistance of asphalt at the corresponding temperature. The greater the viscosity, the greater the shear resistance, and shear failure at high temperature will also be less likely. In order to facilitate mixing and construction, asphalt viscosity should not be too great. In our work, the Brookfield viscosity of each asphalt was determined using the NDJ-1C Brookfield viscometer with an operating temperature range of 0°C~300°C, according to ASTM D 4402. The rotor type was selected as no. 27, and 12.5 g of asphalt was taken for each test. The test temperature ranged from 60°C to 165°C, with 15°C as a temperature interval. The torque range in the test was 10%~98%, and the rotational speed was adjusted according to the test temperature and torque.

2.4. DSR Test. In the late 1980s, the SHRP project introduced the Dynamic Shear Rheometer (DSR) from the material field into civil engineering, thus solving the formlessness issue during asphalt fatigue experiments. Until now, the primary study on asphalt fatigue properties was implemented by the DSR parallel plate. In this study, the HR-1 Dynamic Shear Rheometer (DSR) produced by the TA Company of the United States was used for the temperature and frequency scanning of each asphalt (ASTM D7175). The spacing between the two parallel plates was adjusted to 1 mm, and the trimming gap was 50 μm. The temperature scanning test temperature ranged from 52°C to 76°C, with 6°C as a temperature interval, and the loading angular frequency was 10 rad/s. The frequency scanning test temperature ranged from 58°C to 70°C, with 6°C as a temperature interval, and the loading strain was 5%, while the frequency range was 0.1~100 rad/s.

The G^* and δ are the most important evaluation indexes in temperature scanning and frequency scanning, and the other rheological parameters can be calculated by the following two indexes. Equations (1)~(3) show the relationship between the viscoelastic parameters and G^* and δ.

$$G^* = G' + iG'', \tag{1}$$

$$G' = \left|G^*\right| * \cos\delta, \tag{2}$$

$$G'' = \left|G^*\right| * \sin\delta. \tag{3}$$

3. Results and Discussion

3.1. Viscosity-Temperature Performance. The viscosity of asphalt as a viscoelastic material is closely related to temperature. However, the demand for viscosity of asphalt pavement during construction and service is contradictory. Asphalt mixtures need low viscosity during construction, which allows the mixture to keep flowing and makes it easy to construct. However, in the summer high-temperature season, the temperature of asphalt pavement can reach more than 50°C. Under these conditions, the asphalt mixture needs to maintain a high viscosity in order to reduce high-temperature distress. The viscosity temperature curve can effectively mirror the trend of asphalt viscosity with temperature change, and therefore it was very important to establish a reasonable viscosity-temperature relationship for the construction and normal use of hard petroleum asphalt. The viscosity of each asphalt was measured with a Brookfield rotational viscometer, as shown in Table 2. Based on this, the temperature-viscosity curve and equation were obtained.

Table 2 compares the Brookfield viscosity at eight different temperatures. The viscosity decreased with the increase of temperature, and with the same oil source, it was determined that the higher the asphalt grade, the lower the viscosity. With a different oil source, GF viscosity was greater than KL. However, at the test temperature of 135°C, the viscosity of K2 was greater than G2, a result that may have been caused by human error. Compared with SBSPMA, the hard petroleum asphalt viscosity was lower. In order to reflect the content of the table more intuitively, it was necessary to use the viscosity-temperature relationship equation to further process the data in the diagram and to complete it through the REFUTAS curve.

The REFUTAS curve has been widely used in the area of petroleum asphalt and can be linear in a wide temperature range. The REFUTAS curve equation describes the relationship between viscosity and temperature, as shown in

$$\log\ \log(\eta + 0.8) = m \log K, \tag{4}$$

where η is viscosity, m is a constant, and K is the absolute temperature.

After the constant 0.8 is omitted, the above equation is standardized, and the viscosity-temperature curve expression shown in equation (5) can thus be obtained.

$$\log\ \log\left(\eta \times 10^3\right) = n - m \log(T + 273.13), \tag{5}$$

where η is viscosity, T is Celsius temperature, and m and n are regression coefficients.

As shown in Figure 1, the overall viscosity of hard petroleum asphalt is less than that of S1. The viscosity of S1 had obvious differences from other types of asphalt. Under the same grade, the viscosity of GF was greater than KL, indicating that the road performance of KL was better than that of GF. The higher the asphalt grade, the lower the viscosity at the same oil source.

Table 2: Viscosity of asphalt with different temperature.

Temperature/°C	60	75	90	105	120	135	150	165
K1/Pa s	1085.00	120.00	22.41	6.21	2.02	0.82	0.37	0.21
K2/Pa s	785.00	99.14	21.45	5.64	1.84	0.80	0.32	0.18
G1/Pa s	1095.00	124.21	24.25	6.54	2.24	0.84	0.40	0.23
G2/Pa s	920.00	116.25	21.84	6.01	1.96	0.65	0.35	0.20
S1/Pa s	2960.00	299.50	46.50	12.10	3.80	1.85	0.57	0.31

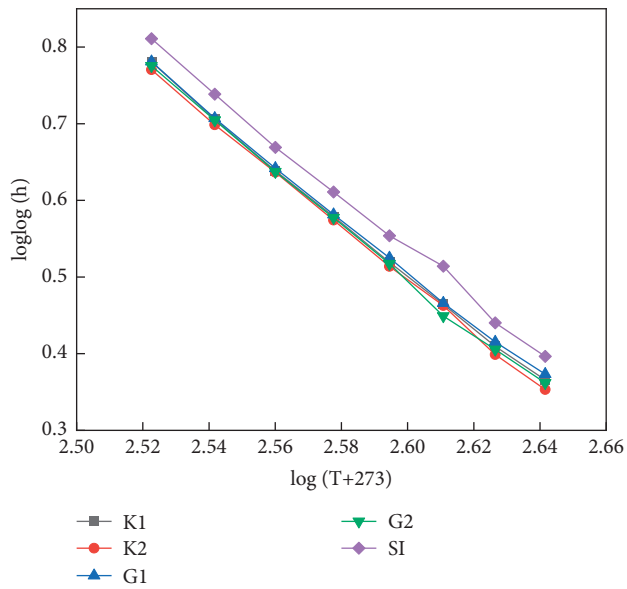

Figure 1: Viscosity-temperature curve.

Table 3 demonstrates the regression results and regression coefficients of the viscosity-temperature curves of each type of asphalt. The regression coefficients of different asphalts were greater than 0.997, indicating that the improved REFUTAS formula was reliable in terms of characterizing the viscosity-temperature relationship of hard petroleum asphalt. The variation trend of the viscosity of each hard petroleum asphalt with temperature was basically the same as S1.

The viscosity-temperature curve allows us to obtain the mixing and compaction temperatures of the hard petroleum asphalt mix. The viscosity levels of $(0.17 \pm 0.02$ Pa-s) and $(0.28 \pm 0.03$ Pa-s) were used as the mixing temperature range and compaction temperature range, respectively, in the viscosity-temperature curve [32–34]. According to the fitting parameters in Table 4, the mixing and compaction temperature ranges of asphalt could be calculated.

Table 4 reports that the construction temperature of asphalt is K2 < G2 < K1 < G1 < S1 and that the construction temperature of hard petroleum asphalt is slightly lower than that of S1. With the same oil source of hard petroleum asphalt, the higher the grade of asphalt, the lower the construction temperature, and for different oil sources of hard petroleum asphalt, KL construction temperature was lower than GF. Also, compared with S1, hard petroleum asphalt was reduced by approximately 10 °C during construction, thus reducing energy consumption and facilitating construction.

Table 3: Viscosity-temperature curve regression results.

Regression coefficient	K1	K2	G1	G2	S1
m	3.488	3.509	3.439	3.521	3.450
n	9.571	9.620	9.450	9.655	9.506
R^2	0.999	0.999	0.999	0.998	0.997

3.2. Temperature Dependence. The temperature dependence of each type of asphalt was studied by using the temperature scanning mode of DSR. The δ and G^* at the same frequency were tested at different temperatures in order to study the effect of temperature and aging degree on the dynamic viscoelastic parameters of hard petroleum asphalt. $|G^*|/\sin\delta$ was calculated by the previously mentioned two parameters in order to characterize the high-temperature resistance to the permanent deformation of asphalt.

3.2.1. Complex Shear Modulus. The G^* represents the resistance of asphalt under dynamic shear deformation and also reflects the deformation resistance of the material. The smaller the G^* value, the worse the ability to resist the deformation of asphalt. Figure 2 shows the G^* changes with the temperatures of five asphalts under different aging conditions.

All of the asphalts in Figure 2 experience similar changes at different test temperatures, and they are different from each other in values. The G^* of K2, G2, and S1 decreased first and then tended to be stable with increased temperature. The ability to resist the deformation of GF and KL reaches the level of S1. Due to the influence of the oil source, G^* of the hard petroleum asphalt with the same grade varies greatly, and the result of the comparison was K2 > G2, but G1 > K1. And with different asphalt from the same oil source, the smaller the grade, the greater the G^* of asphalt. The G^* of hard petroleum asphalt was greater than that of other asphalt, and the total resistance was the highest under repeated shear deformation.

The G^* decreased continuously with increasing temperature, whether the asphalt was described before or after the aging process. This indicated that the rutting resistance of asphalt deteriorated with increasing temperature. At the same test temperature, the G^* increased just as the degree of aging increased, indicating that aging causes the asphalt to change from soft to hard. The reason for this was the volatilization of light components and the generation of strong polar substances during the aging process. The change of G^* of G1 before and after aging was the greatest, and taking the initial temperature of 52 °C as an example, the G^* of asphalt increased by approximately 140% after RTFOT aging and 340% after PAV aging. At the same time, the slope of the G^*

Table 4: Construction temperature.

Temperature/°C	K1	K2	G1	G2	S1
Mixing temperature	165~171	163~169	167~173	164~170	175~181
Compaction temperature	154~158	152~157	156~161	153~158	164~169

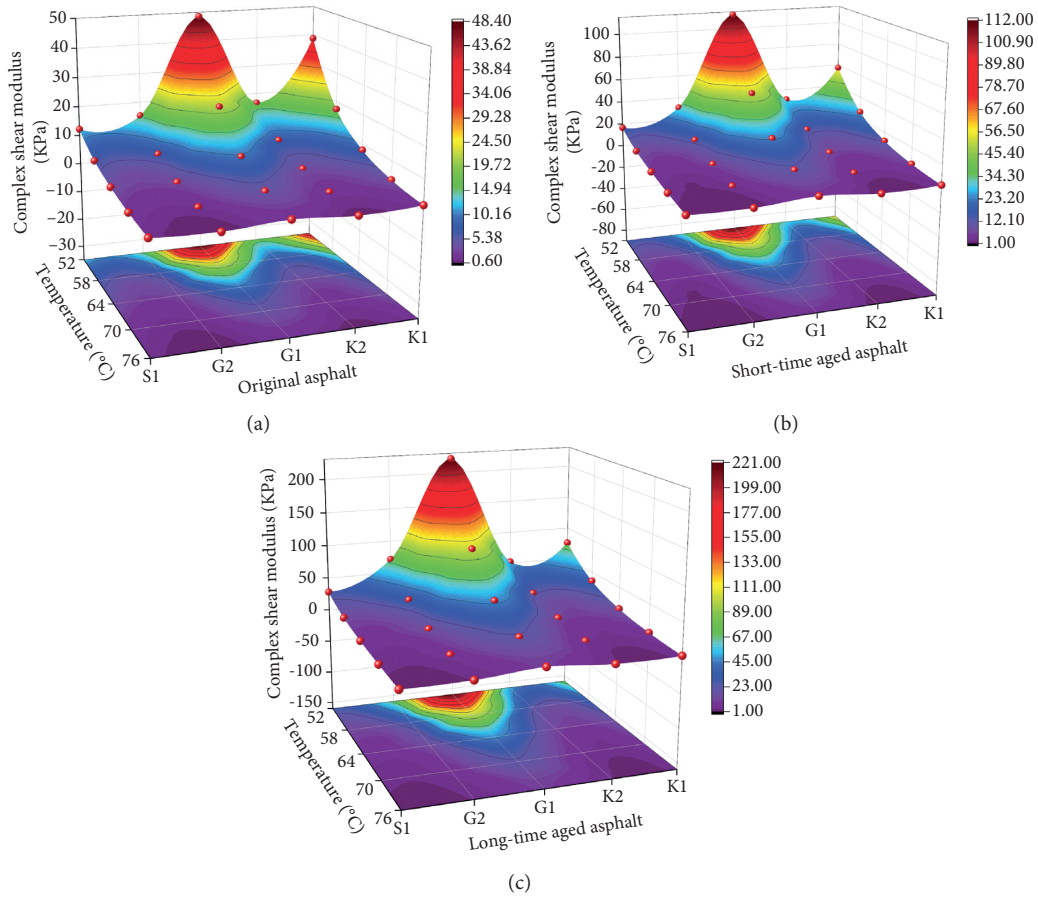

Figure 2: G^* at different aging states. (a) Original asphalt. (b) Short-time aged asphalt. (c) Long-time aged asphalt.

curve gradually increased with increased aging, and the temperature sensitivity of hard petroleum asphalt increased, where G1 had the greatest temperature sensitivity. Moreover, by comparing the maximum and minimum values of G^* before and after aging, it was found that long-term aging had the greatest impact on the G^* of hard petroleum asphalt.

3.2.2. Phase Angle. In dynamic rheological mechanics, the δ characterizes the ratio of viscosity to elasticity in materials. For a complete elastic material with no phase lag of stress and strain, $\delta = 0^\circ$. Correspondingly, for a complete viscous material with a constant phase lag of stress and strain response, $\delta = 90^\circ$. Thus, the phase lag of stress and strain response for viscoelastic material was between 0° and 90°[34]. The δ of KL, GF, and SBSPMA with different aging degrees are shown in Figure 3.

Figure 3 shows that the δ of asphalt in different states are greater than 45°C, thus indicating that each asphalt showed a viscous state in the test temperature range. δ of the five asphalts before and after aging gradually increased as the temperature increased, which indicates that the viscous components of asphalt increased and the elastic components decreased with the increase of temperature. For hard petroleum asphalt with different oil sources, the viscosity of G1 was smaller than that of K1, while the viscosity of G2 was larger than that of K2. This indicates that asphalt from different oil sources exhibited different changes in viscoelastic properties with changes in the hard petroleum asphalt grade. And for asphalt from the same oil source, the greater the grade, the higher the viscosity ratio. The δ of KL and GF under different aging conditions was greater than that of S1 due to the fact that the viscoelastic properties of S1 were stable under different test temperatures. Additionally, the δ of each hard petroleum asphalt decreased the test temperature as aging increased. This indicates that aging increases the elasticity of the hard petroleum asphalt, decreases the viscosity, increases the stability of the colloidal structure, decreases the temperature sensitive properties, and strengthens the deformation resistance.

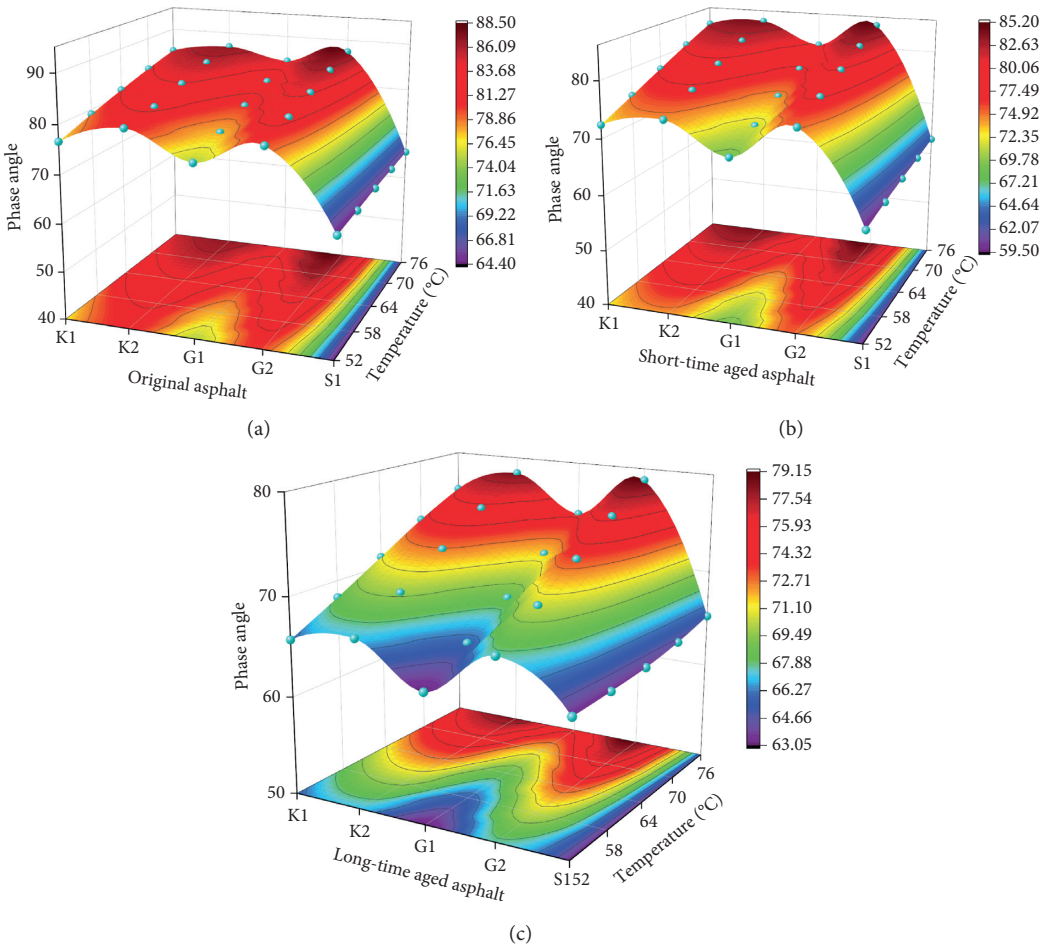

Figure 3: Phase angle at different aging states. (a) Original asphalt. (b) Short-time aged asphalt. (c) Long-time aged asphalt.

3.2.3. Rutting Factor. $|G^*|/\sin\delta$ can be obtained by G^* and δ. $|G^*|/\sin\delta$ reflects the high-temperature deformation resistance of asphalt. The higher its value, the stronger deformation resistance. The $|G^*|/\sin\delta$ of five asphalts under different aging degrees are listed in Figure 4.

Figure 4 lists $|G^*|/\sin\delta$ of five kinds of asphalt before and after aging decrease with the increase of temperature, indicating that the increase of temperature caused the rutting resistance of each asphalt to decrease. Compared with the hard petroleum asphalt from different oil sources, the rutting factor of K1 was smaller than that of G1 in each state, while the rutting factor of G2 at each temperature was gradually greater than that of K2 with the deepening of aging, indicating that GF has a strong antiaging ability. The rutting factor of G1 decreased most obviously as the temperature increased, indicating that the rutting stability of G1 was poorer than that of other asphalts. With the increase of aging degree, the change trend of the rutting factor of K1 was gradually flat, and its high-temperature performance was stable. The decreasing trend of the rutting factor of K2 and G2 was basically the same as that of S1.

Combined with the information from Table 1, it could be concluded that the rutting factor was negatively correlated with the penetration by comparing the rutting factor and the penetration of asphalt in various states. Due to the low penetration of G1, it was shown to have greater advantages in terms of its antirutting ability. As aging made the components of asphalt more stable, $|G^*|/\sin\delta$ of each asphalt was relatively close. This fully reflects the relationship between the deformation resistance of asphalt and temperature. Under different temperatures and different aging degrees, hard petroleum asphalt had a higher rutting resistance than S1, and this also proved that hard petroleum asphalt had better deformation resistance than S1.

3.2.4. Temperature Sensitivity. Because asphalt is a viscous temperature characteristic material, its sensitivity to temperature is particularly important to note. The temperature sensitivity of asphalt can be realized by the complex modulus index (GTS) method. The greater the GTS value, the higher the temperature sensitivity of asphalt [35]. The calculation formula of GTS is shown in

$$\lg\lg G^* = \mathrm{GTS} \times \lg T + c. \tag{6}$$

The temperature sensitivity of asphalt with different aging degrees was measured in the temperature range of 52~76°C. Figure 5 shows the double logarithmic curve of G^*

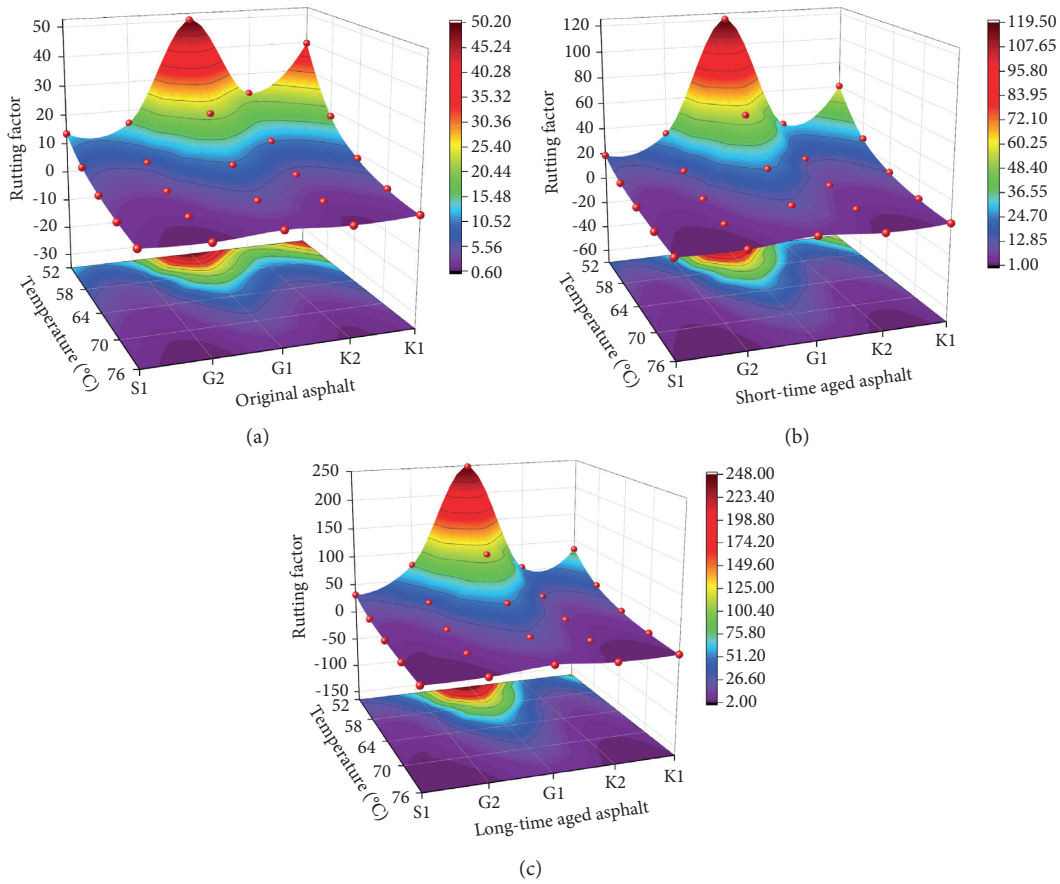

Figure 4: Rutting factor at different aging states. (a) Original asphalt. (b) Short-time aged asphalt. (c) Long-time aged asphalt.

of each asphalt changing with temperature. Table 5 shows the GTS value of each asphalt and the corresponding regression formula.

Table 5 lists the GTS values and regression coefficients of different aged asphalts. The regression coefficients of different asphalts were greater than 0.985, indicating that the G^* data of hard petroleum asphalt tested by the DSR test were relatively stable. The GTS method was reliable in terms of characterizing the temperature sensitivity of hard petroleum asphalt. Compared with asphalt samples of different aging states, the GTS value of hard petroleum asphalt decreased gradually with the deepening of aging. In addition, the GTS value of asphalt from the same oil source increased as the grade increased. There was no obvious pattern of GTS variation for asphalts of different oil sources due to the influence of the oil source. Comparing the hard asphalt with different oil sources, the GTS value of K2 was less than that of G2 in all states. While the GTS value of K1 was greater than that of G1 before aging, the GTS value of K1 was less than that of G1 after aging, which indicated that the overall temperature sensitivity of KL hard asphalt was lower than that of GF hard asphalt. Due to the role of the modifier GTS value, S1 was small, and with the increase of aging degree, there was no obvious rule. The GTS values of GF and KL were greater than those of S1 under different aging conditions, indicating a higher temperature sensitivity.

In terms of an analysis of its causes, the presence of wax made the asphalt reduce at high-temperature viscosity. Low temperature due to the formation of wax crystalline skeleton asphalt rheology characteristics became poor. Thus, it has been shown that the presence of wax would improve the temperature sensitivity of asphalt at high temperatures. In addition, for different varieties of asphalt, the molecular weight also affects its temperature sensitivity. If the intermolecular force is strong, and the relative displacement of molecular chain segments or the possibility of molecular movement is small, then the asphalt temperature sensitivity is also small [36]. In general, the deepening of aging can improve the temperature sensitivity of hard petroleum asphalt in high-temperature regions.

3.3. Time Dependence. G^* and δ values were obtained through the use of frequency scan DSR tests. Furthermore, the time dependence of each asphalt at different temperatures and frequencies was also investigated. The influence of aging on the time dependence of hard petroleum asphalt was determined by comparing asphalt samples with different degrees of aging.

3.3.1. Complex Shear Modulus. The curves of G^* of asphalt with different aging degrees at different temperatures with the change of loading frequency are shown in Figure 6.

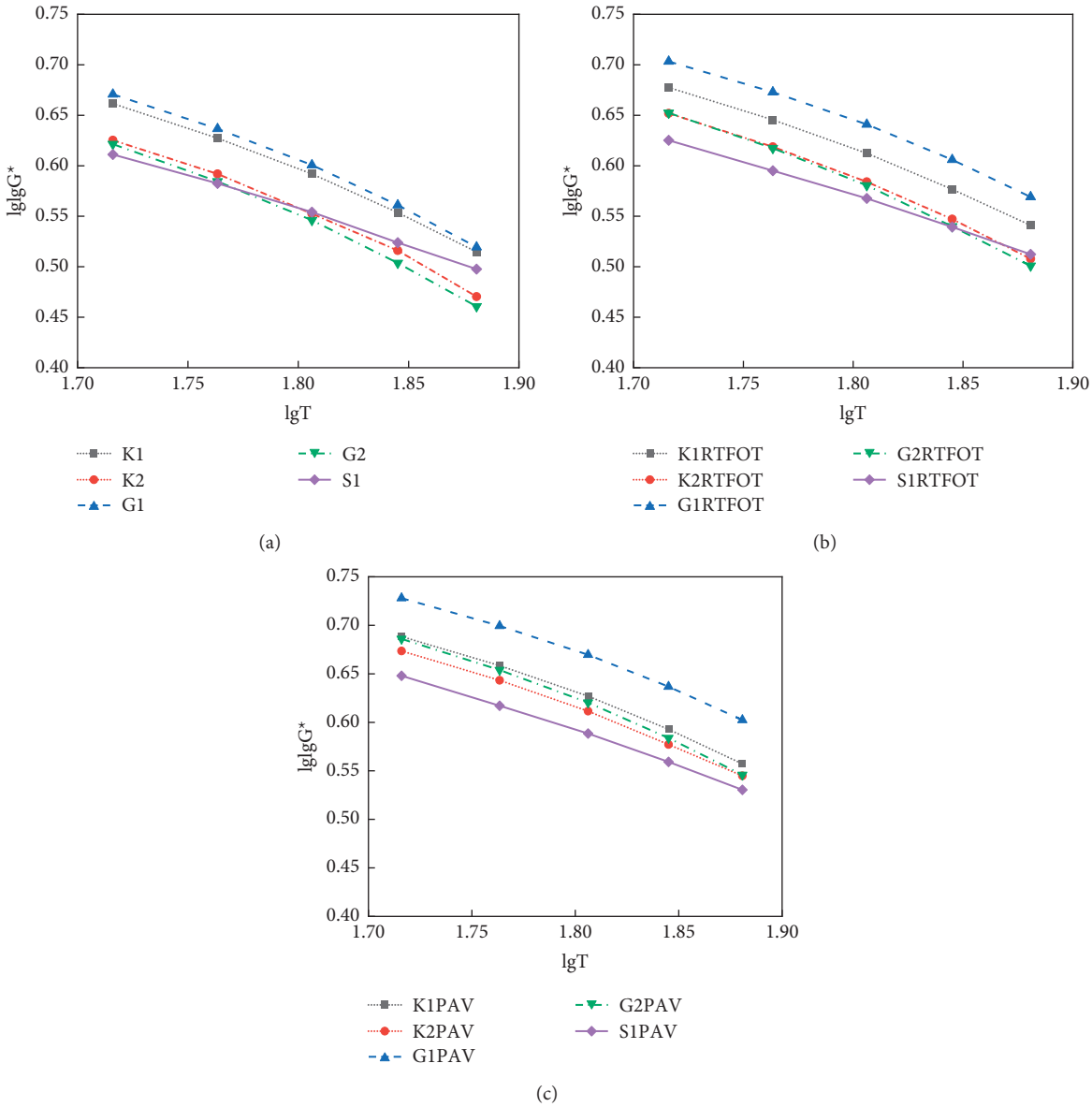

Figure 5: The relationship between the double logarithm of G^* and temperature. (a) Original asphalt. (b) Short-time aged asphalt. (c) Long-time aged asphalt.

It is apparent from Figure 6 that with the increase of scanning frequency, G^* of each asphalt increases gradually, and the total resistance generated by repeated shear deformation increases. The higher the temperature, the lower the G^* of the sample, and the smaller the total resistance produced by repeated shear deformation. At the same temperature, with the increase of aging degree, G^* of each asphalt sample decreased. In addition, due to the influence of the oil source, the influence of aging on low-temperature high-frequency and high-temperature low-frequency of GF was greater than that of KL. The G^* of S1 was less than that of KL and GF. As the angular frequency increased, the smaller the asphalt grade of the same oil source became and the greater the G^*. At the same time, with the gradual increase of scanning frequency, the difference of G^* under different temperature conditions gradually increased. This indicated that the total resistance to repeated shear deformation of hard graded asphalt varied more with increasing loading frequency under different ambient temperature conditions. We compared the variation pattern of G^* of each asphalt under the most unfavorable conditions of load action (i.e., angular frequency of 100 rad/s). Comparing hard petroleum asphalt with different oil sources, it was found that G^* of KL hard asphalt was less than that of GF hard asphalt at the same temperature and aging state. When the oil source was the same, there was no obvious pattern in the variation of G^* of each asphalt with the grade.

Under the same temperature conditions, G^* of asphalt increased with the increase in load frequency, indicating that the viscoelastic properties of asphalt tended towards elastic behavior at higher load frequencies. The asphalt

Table 5: Asphalt GTS value and regression equation.

Asphalt type	GTS	Regression formula	R^2
K1	0.889	$y = -0.889x + 2.192$	0.990
K2	0.932	$y = -0.932x + 2.232$	0.985
G1	0.915	$y = -0.915x + 2.246$	0.987
G2	0.973	$y = -0.973x + 2.298$	0.989
S1	0.693	$y = -0.693x + 1.803$	0.997
K1RTFOT	0.827	$y = -0.827x + 2.102$	0.991
K2RTFOT	0.871	$y = -0.871x + 2.151$	0.989
G1RTFOT	0.811	$y = -0.811x + 2.100$	0.988
G2RTFOT	0.920	$y = -0.920x + 2.237$	0.991
S1RTFOT	0.683	$y = -0.683x + 1.799$	0.998
K1PAV	0.794	$y = -0.794x + 2.056$	0.989
K2PAV	0.783	$y = -0.783x + 2.022$	0.992
G1PAV	0.759	$y = -0.759x + 2.035$	0.988
G2PAV	0.847	$y = -0.847x + 2.145$	0.989
S1PAV	0.711	$y = -0.711x + 1.840$	0.997

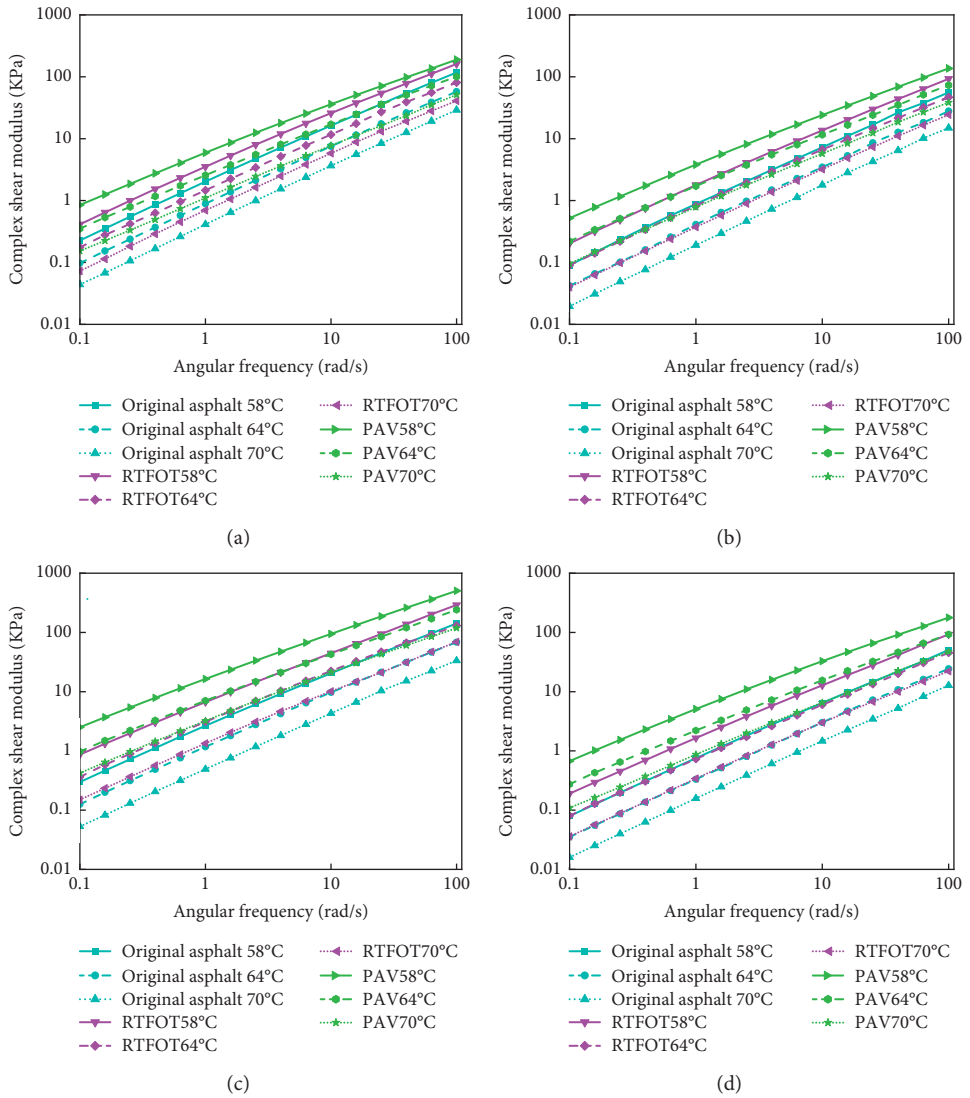

Figure 6: Continued.

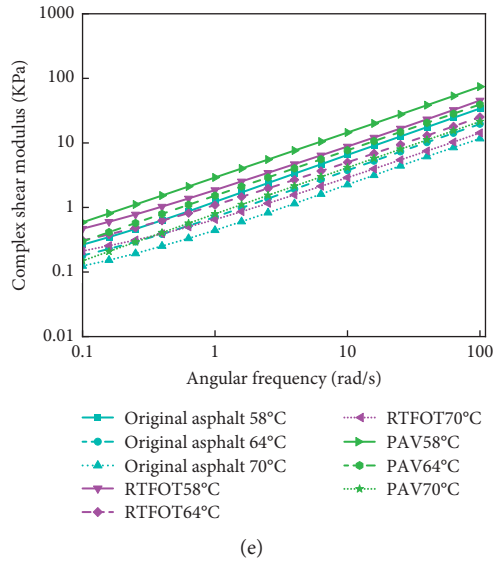

(e)

Figure 6: Frequency sweep G^* curve of each asphalt. (a) K1. (b) K2. (c) G1. (d) G2. (e) S1.

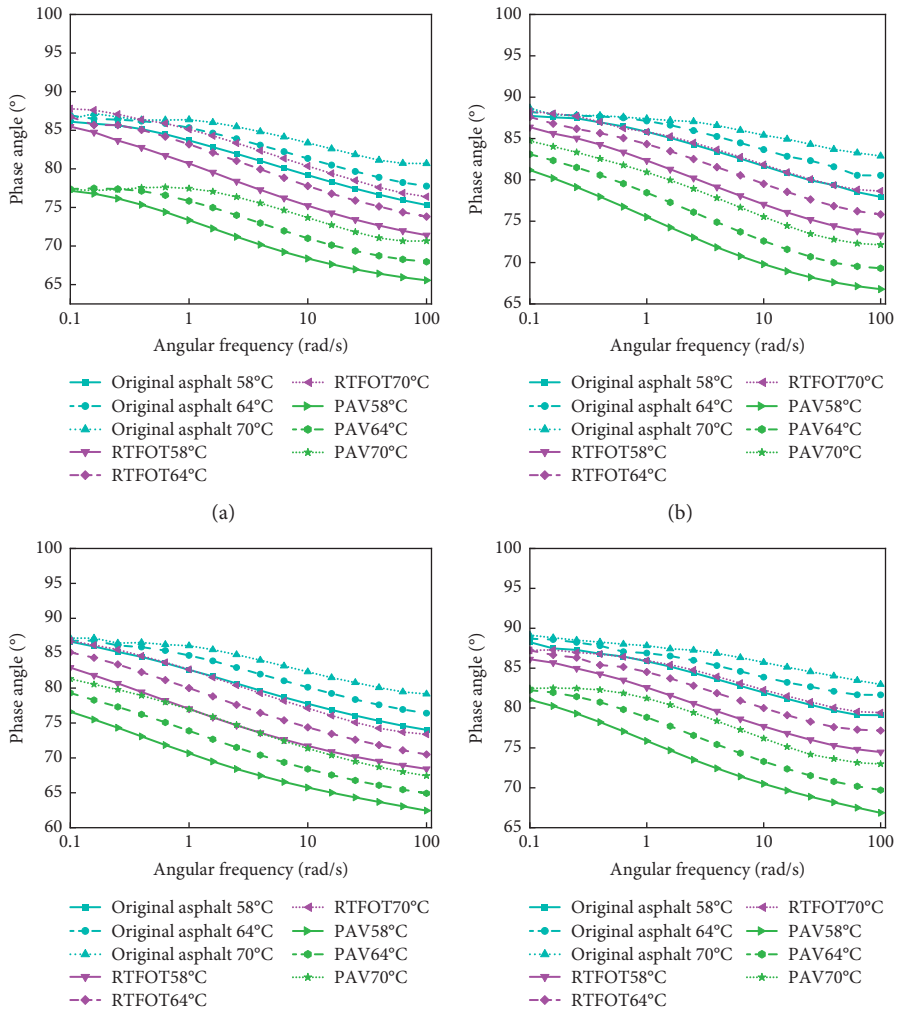

(a) (b) (c) (d)

Figure 7: Continued.

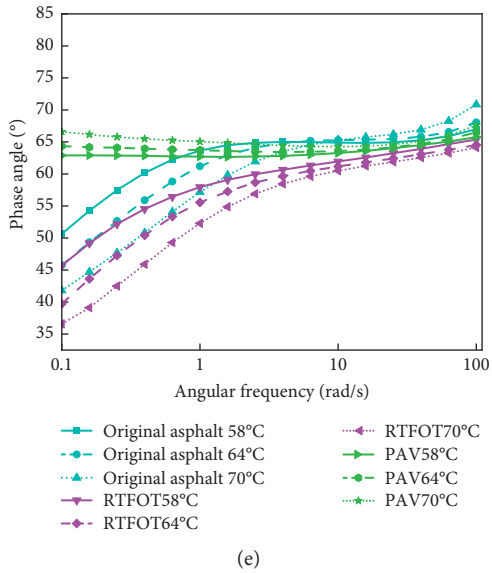

(e)

Figure 7: Frequency sweep phase angle of each asphalt. (a) K1. (b) K2. (c) G1. (d) G2. (e) S1.

material had a better recovery from deformation and could better resist deformation at high temperatures. Comparing KL, GF, and S1 under the same temperature conditions, G^* of KL and GF were greater than that of S1, which meant that the elastic properties of hard petroleum asphalt under the same conditions were better than S1 elastic properties. Thus, hard petroleum asphalt had better deformation recovery ability, and it had stronger resistance to rutting deformation as well.

3.3.2. Phase Angle. Figure 7 presents the δ of asphalt with different aging degree changes with the load frequency at different temperatures.

Figure 7 demonstrates that with the increase of temperature and the decrease of frequency, δ of hard petroleum asphalt increased. Under the same test temperature and scanning frequency, δ of hard petroleum asphalt was decreased as the aging degree increases. δ of hard petroleum asphalt under each aging state had no change with the attenuation trend of scanning frequency. Following an analysis of asphalt from different oil sources, δ of G1 was found to be less than that of other hard petroleum asphalt at the same frequency and temperature, indicating that there were more elastic components in G1. For asphalt from the same oil source, δ increased with the increase of hard petroleum asphalt label. δ of S1 increased as the scanning frequency increased, and δ of S1 increased as the temperature increased in the original sample and PAV aging state, but the overall change was small. This indicated that the elastic component of S1 was relatively stable. In general, when the frequency was in the range of 0.1–100 rad/s, δ of hard petroleum asphalt and S1 presented different rules with regards to frequency. At a lower frequency, the elastic component of S1 was better than that of hard petroleum asphalt, but at a higher frequency, the elastic component of hard petroleum asphalt was equivalent to S1.

4. Conclusion

The high-temperature viscoelastic properties of hard petroleum asphalt and S1 in their original state, as well as in different aging states, were investigated by Brookfield viscosity tests, temperature scan tests, and frequency scan tests. The main conclusions were as follows:

(1) The improved REFUTAS equation can better characterize the hard petroleum asphalt viscosity-temperature relationship with a correlation coefficient greater than 0.997. KL also exhibits better workability compared to S1 and can reduce the construction temperature by approximately 10°C.

(2) Compared to S1, hard petroleum asphalt had a higher G^*. At the same time, aging has a greater impact on G^* of GF at low-temperature high-frequency and high-temperature low-frequency conditions.

(3) The hard petroleum asphalt has higher rutting resistance compared to S1 at different temperatures and aging conditions. Among the four hard petroleum asphalts, the antirutting ability of G1 decreases most with temperature, but still has good antirutting ability.

(4) The correlation coefficients of each asphalt's G^* and temperature change curve obtained by the GTS method were greater than 0.985. This can better describe the sensitivity of hard petroleum asphalt to temperature. Also, the temperature sensitivity of hard petroleum asphalt decreased with increased aging.

Data Availability

The data used to support the findings of this study are included within the article.

Conflicts of Interest

All authors confirm that there are no conflicts of interest in this research article.

Acknowledgments

The authors gratefully acknowledge the financial supports by the National Natural Science Foundation of China (51408287, 51668038, and 51868042), the Distinguished Young Scholars Fund of Gansu Province (1606RJDA318), the Natural Science Foundation of Gansu Province (1506RJZA064 and 20JR10RA227), Industry Support and Guidance Project by University and College in Gansu Province (2020C-13), and Foundation of A Hundred Youth Talents Training Program of Lanzhou Jiaotong University and Research Institute of PetroChina Fuel Oil Co.

References

[1] X. Wang, *Research on Preventive Maintenance Decision of Expressway Asphalt Pavement*, Dalian University of Technology, Dalian, China, 2020.

[2] Q. Cao, *Rutting Analysis of Influencing Factors of Asphalt Pavement based on Temperature Field*, Shijiazhuang Tiedao University, Shijiazhuang, China, 2020.

[3] Y. Yi, *Research and Application of High Temperature Stability of Asphalt Mixture under High Temperature and Heavy Load*, Southeast University, Nanjing, China, 2019.

[4] L. Jia, *Rutting Predication of Asphalt Pavement Based on Total-Thickness Rutting Test*, Huazhong University of Science and Technology, Wuhan, China, 2015.

[5] A. K. KumarSingh and J. P. Sahoo, "Rutting prediction models for flexible pavement structures: a review of historical and recent developments," *Journal of Traffic and Transportation Engineering*, vol. 8, no. 3, pp. 315–338, 2021.

[6] B. Yi, *Evaluation Method of High Temperature Stability of Asphalt Mixture*, Suzhou University of Science and Technology, Suzhou, China, 2019.

[7] Q. Song, *Study on the Hard Paving Grade Asphalt Binder and Mixtures*, Chang'an University, Xi'an, China, 2015.

[8] E. Behzadfar and S. G. Hatzikiriakos, "Viscoelastic properties and constitutive modelling of bitumen," *Fuel*, vol. 108, pp. 391–399, 2013.

[9] M. Espersson, "Effect in the high modulus asphalt concrete with the temperature," *Construction and Building Materials*, vol. 71, pp. 638–643, 2014.

[10] H. Geng, C. S. Clopotel, and H. U. Bahia, "Effects of high modulus asphalt binders on performance of typical asphalt pavement structures," *Construction and Building Materials*, vol. 44, pp. 207–213, 2013.

[11] Q. He, "research on damage characteristics and preventive maintenance measures of expressway asphalt pavement," *Construction & Design for Engineering*, vol. 19, pp. 94–96, 2019.

[12] Y. Chen, C. Ji, and H. Wang, "Evaluation of crumb rubber modification and short-term aging on the rutting performance of bioasphalt," *Construction and Building Materials*, vol. 193, pp. 467–473, 2018.

[13] R. Zhang and Y. Huang, "Review on influence of rigid asphalt and asphalt temperature index," *International Journal of Civil Engineering and Machinery Manufacture*, vol. 5, no. 1, pp. 115–123, 2020.

[14] Z. Dong, G. Xiao, and X. Gong, "Analysis on impact of gradation and anti-rutting additive on rutting resistance of asphalt mixture," *Journal of Highway and Transportation Research and Development*, vol. 31, no. 2, pp. 27–31, 2014.

[15] X. Zou, A. Sha, and W. Jiang, "Modification mechanism of high modulus asphalt binders and mixtures performance evaluation," *Construction and Building Materials*, vol. 90, pp. 53–58, 2015.

[16] C. Han, *Application Research on Durable High Modulus Asphalt Mixture Design Using Hard Paving Bitumen*, Southeast University, Nanjing, China, 2018.

[17] S. F. Brown, J. M. Brunton, and A. F. Stock, "The analytical design of bituminous pavements," *Proceedings - Institution of Civil Engineers*, vol. 79, no. No. 1, pp. 1–31, 1985.

[18] M. E. Nunn, A. Brown, and D. Weston, *Design of Long-Life Flexible Pavements for Heavy Traffic*, Transport Research Laboratory, Berkshire, USA, 1997.

[19] D. E. Newcomb, M. Buncher, and I. J. Huddleston, *Concepts of Perpetual Pavements*, TRB, National Research Council, Washington (DC), 2001.

[20] I. Hafeez, M. A. Kamal, and W. Mirza, "Domains of permanent deformation coefficient alpha and mu for hard grade asphalt concrete mixtures," *Proceedings of Pakistan Academic Science*, vol. 47, pp. 65–74, 2010.

[21] B. Garba, *Permanent Deformation Properties of Asphalt concrete Mixtures*, Norwegian University of Science and Technology, Oslo, Norway, 2002.

[22] M. P. Mwangi, *Permanent Deformation of Asphalt Mixtures," Section of Road and Railway Engineering*, pp. 35–56, Faculty of Civil Engineering and Geosciences, Delft University of Technology, Netherlands, 2007.

[23] H. Zhu and J. Yang, "Comparative analysis of rutting resistance of hard-grade Asphalt," *Journal of China & Foreign Highway*, vol. 6, pp. 214–216, 2006.

[24] W. Ouyang, G. Yu, and F. Zhu, "Research on anti-rutting performance of high modulus asphalt concrete pavement," *Advanced Materials Research*, vol. 1067, pp. 4474–4477, 2010.

[25] C. Wu, B. Jing, and X. Li, "Performance evaluation of highmodulus asphalt mixture," *Advanced Materials Research*, vol. 311–313, pp. 2138–2141, 2011.

[26] F. Dong, X. Yu, and S. Liu, "Rheological behaviors and microstructure of SBS/CR composite modified hard grade asphalt," *Construction and Building Materials*, vol. 115, pp. 285–293, 2016.

[27] C. Xin, Q. Lu, and C. Ai, "Optimization of hard modified asphalt formula for gussasphalt based on uniform experimental design," *Construction and Building Materials*, vol. 136, pp. 556–564, 2017.

[28] A. Sha, J. Cao, and Q. Zhou, "High temperature performance of domestic hard grade asphalt and asphalt mix," *Journal of Wuhan University of Technology*, vol. 31, no. 1, pp. 41–44, 2009.

[29] W. Wang, D. Ma, and C. Fan, "Rheological property and comparison of high-temperature performance of hard-grade Asphalt before and after aging," *Journal of Chongqing Jianzhu University*, vol. 36, no. 6, pp. 48–52, 2017.

[30] JTG E20-2011, *Standard Test Methods of Bitumen and Bituminous Mixtures for Highway Engineering*, China Communications Press, Beijing, China, 2011.

[31] X. Jia, *Study on Performance of Rubber Powder/sbs Composite Modified Asphalt and Mixture*, Lanzhou Jiaotong University, Lanzhou, China, 2020.

[32] Z. Liu, Q. Sha, and Z. Li, "Experimental investigation on property of hard grade asphalt A-30 and asphalt mixture," *Petroleum Asphalt*, vol. 22, no. 2, pp. 7–13, 2008.
[33] Z. Hu, *Research on Technical Index of Grade Hard Grade Asphalt and Pavement Performance of its Mixture*, South China University of Technology, Changsha, China, 2011.
[34] Y. Dong and Y. Tan, "Research on high temperature performance of hard grade Asphalt based on repeated shear creep test," *Highways*, vol. 60, no. 2, pp. 160–164, 2015.
[35] Z. Zhang, B. Li, and X. Ren, "research on thermal aging properties of microwave crumb rubber modified asphalt," *Journal of Materials Science and Engineering*, vol. 37, no. 6, pp. 1001–1007, 2019.
[36] L. Wang, J. Hu, G. Chen, Y.-J. Jia, and Y. Wang, "Temperature susceptibility of different kings of modified asphalt," *Journal of Functional Materials*, vol. 46, no. 4, pp. 4086–4090, 2015.